



**HAL**  
open science

## Order and disorder at the C-face of SiC: A hybrid surface reconstruction

Eduardo Machado-Charry, César González, Yannick Dappe, Laurence Magaud, Normand Mousseau, Pascal Pochet

► **To cite this version:**

Eduardo Machado-Charry, César González, Yannick Dappe, Laurence Magaud, Normand Mousseau, et al.. Order and disorder at the C-face of SiC: A hybrid surface reconstruction. Applied Physics Letters, 2020, 116 (14), pp.141605. 10.1063/1.5143010 . hal-03013195

**HAL Id: hal-03013195**

**<https://hal.science/hal-03013195v1>**

Submitted on 18 Nov 2020

**HAL** is a multi-disciplinary open access archive for the deposit and dissemination of scientific research documents, whether they are published or not. The documents may come from teaching and research institutions in France or abroad, or from public or private research centers.

L'archive ouverte pluridisciplinaire **HAL**, est destinée au dépôt et à la diffusion de documents scientifiques de niveau recherche, publiés ou non, émanant des établissements d'enseignement et de recherche français ou étrangers, des laboratoires publics ou privés.

**Order and disorder at the C-face of SiC: an hybrid surface reconstruction**

Eduardo Machado-Charry,<sup>1</sup> Cesar Gonzalez Pascual,<sup>2</sup> Yannick J. Dappe,<sup>3</sup> Laurence Magaud,<sup>4</sup> Normand Mousseau,<sup>5</sup> and Pascal Pochet<sup>6</sup>

<sup>1</sup>*Institute of Solid State Physics and NAWI Graz, Graz University of Technology, Petersgasse 16, 8010 Graz, Austria*

<sup>2</sup>*Departamento de Fisica Teorica de la Materia Condensada and Condensed Matter Physics Center, Facultad de Ciencias, Universidad Autonoma de Madrid, E-28049 Madrid, Spain*

<sup>3</sup>*SPEC, CEA, CNRS, Université Paris-Saclay, CEA Saclay, 91191 Gif-sur-Yvette Cedex, France*

<sup>4</sup>*Université Grenoble Alpes, CNRS, Institut Neel, F-38042 Grenoble, France*

<sup>5</sup>*Département de Physique and RQMP, Université de Montréal, Case Postale 6128, Succursale Centre-ville, Montréal, Québec H3C 3J7, Canada*

<sup>6</sup>*Department of Physics, IriG, Univ. Grenoble Alpes and CEA, F-38000 Grenoble, France*

(Dated: 17 December 2019)

In this letter, we explore the potential energy surface (PES) of the  $3\times 3$  C-face of SiC by means of density functional theory. Following an extensive and intuitive exploration, we propose a model for this surface reconstruction based on an all-silicon over-layer forming an ordered honeycomb-kagome network. This model is compared to the available experimental Scanning Tunneling Microscope (STM) topographies and conductance maps. Our STM simulations reproduce the three main characteristics observed in the measurements, revealing the underlying complex and hybrid passivation scheme. Indeed, below the ordered over-layer, the competition between two incompatible properties of silicon induces a strong disorder in the charge transfer between unpassivated dangling bonds of different chemistry. This effect, in conjunction with the glassy-like character of the PES, explain why it took decades to explain this structure.

Semiconductor surfaces reconstruct mainly through ad-atoms either self-reorganization.<sup>1</sup> In the former, the dangling bonds are passivated by forming new bonds with the additional atoms, while in the latter, the dangling bonds are partially or completely eliminated via some charge transfer. Although reconstructions usually follow one or the other scheme, both mechanisms are sometimes mixed. In most cases, a hybrid mechanism takes place when some unpassivated surface atoms (known as *rest* atoms<sup>1</sup>) undergo a charge transfer with the ad-atoms. As a consequence, the surface can exhibit a commensurate and ordered super-structure. A deep understanding of these reconstruction mechanisms is central in applied physics and, more particularly, for growth science as well as for tuning new devices based on the use of interfacial physics such as 2D electron gas or surface superconductivity.<sup>2</sup>

Though being of relative importance for the growth of graphene from hexagonal SiC, a reconstruction at the carbon face ( $000\bar{1}$ ) surface (known as  $3\times 3$ ) has remained unresolved for more than two decades. We show in the following that it corresponds to a hybrid reconstruction, in which an ordered network of ad-atoms and a partial intermixing at the level of the rest-atoms lead to a hybrid incommensurate and ordered structure.

The  $3\times 3$  was first imaged by means of Scanning Tunneling Microscopy (STM) in 1997.<sup>3</sup> This system shows a clear distinction between STM features at occupied states ( $stm_o$ ) and unoccupied states ( $stm_u$ ). Several attempts<sup>3-7</sup> to explain these observations with an atomic model of the surface were unsuccessful since the exact composition of the surface as well as the affected number of layers cannot be attained from the experimental data. The difficulty of determining the composition of the bare  $3\times 3$  is increased as this surface undergoes an evolution by increasing the temperature, with the subsequent formation of graphene on it.<sup>8</sup> In 2012, cutting-edge STM data<sup>5,9</sup> revealed new features ( $stm_g$ ) at an energy range close to zero bias. The three distinct STM features of the  $3\times 3$  are reproduced in Fig. 1(a-c). Following the notation in Ref. 3, these features are explained in terms of three symmetry points of the surface cell, namely *A*, *B* and *C*; at  $(\frac{1}{3}, \frac{1}{3})$ ,  $(\frac{2}{3}, \frac{2}{3})$  and  $(1, 1)$  respectively. The  $stm_o$  shows a simple kagome-like pattern where sites *A* and *B*, at the center of each triangle, have the same intensity and are equivalent by rotation. This equivalence is broken at  $stm_u$  where only at sites *A* a clear wide spot is visible in the surface cell. On the other hand, sites *C* show low intensity values in  $stm_o$  and  $stm_u$ . However, the picture is quite different at low bias, i.e.  $stm_g$  [Fig. 1(c)], where only signal from some *C* sites is observed when analyzing conductance images of several adjacent surface cells. Bright and dark signals at *C* sites (labeled  $C^+$  and  $C^-$ ) appear without any clear order. The analysis of different images shows that the  $C^+$  sites represent

between 60% and 70% of the total number of  $C$  sites.<sup>5</sup>

This puzzling situation motivates us to explore the potential energy surface (PES) for this system in order to identify the structure. An exhaustive search for the PES, with methods such as ART<sup>10</sup> is, however, not possible today for two main reasons. First, with both silicon and carbon easily adopting complex structures, the PES of the SiC surface is complex, almost glassy-like in character.<sup>11</sup> This suggests that a complete exploration of the landscape would require sampling a large number of states, many accessible only through highly non-equilibrium pathways. Second, and more important, the PES exploration must take place in the grand canonical ensemble and current systematic exploration tools are not able to treat this ensemble efficiently. In view of these limitations, we select to pursue an extensive manual search mainly driven by user intuition and comparison spanning over a large range of surface concentration as depicted in Fig. 2(a). Energy optimization for all the configurations are determined using BigDFT with surface conditions<sup>12</sup> in a  $3 \times 3$  orthorhombic cell containing four SiC bilayers stacked in  $4H$ , the silicon atoms of the bottom bilayer being hydrogen passivated. The LDA functional and 2 k-points in the zigzag direction are used in addition to standard parameters.<sup>10</sup> Based on the surface formation energy ( $FE$ ) plot, selected configurations (see below) are further analyzed with FIREBALL package<sup>13</sup> for extracting the hamiltonian partial DOS for the STM simulation with a home-made code, using a realistic W-tip.<sup>14</sup>

In 2015, while analyzing new STM topographies for ultra-thin silicon dioxide layer grown on  $2 \times 2$  Ru oxide,<sup>15</sup> we identified some similarities between both systems. Figures 1(a) and 1(d) show that there is a clear correspondence between the  $stm_o$  of the  $3 \times 3$  and the STM image of the silica ad-layer on Ru oxide. Both show a kagome network, the only difference being that the  $C$  site is always bright in the latter. Although both images were taken at different polarity, the known configuration of the silica ( $Si_2O_3$ ) on Ru oxide [Figs. 1(e-f)] is used as a template for the  $3 \times 3$ . Thus, we simply *transmute* each bridging oxygen of the silica into a bridging silicon atom. This results in an almost flat over-layer made of five silicon ad-atoms [Figs. 1(g-h)]. Due to its two dimensional character this model is called  $2DL_1$  in our exploration nomenclature [Fig. 2(b)]. As can be seen in Figs. 1(i-j) the simulated STM images based on the  $2DL_1$  model nicely reproduce both  $stm_o$  and  $stm_u$ . Through careful scrutiny of these images, sites  $A$  and  $B$  in Figs. 1(a-b) can be identified with the two non-bridging silicon atoms, i.e. with the two silicon atoms of the silica model forming a honeycomb network. On the other hand, the three bridging silicon atoms are responsible for the bright STM features in the kagome pattern, as the bridging O atoms do for

silica [Fig. 1(d)]. We will refer to these bridging sites as *O* sites in the following.

The  $2DL_1$  over-layer, despite the previous results, fails to reproduce the third STM condition, i.e.  $stm_g$ . This discrepancy is a weak but is yet a clear signal that something is still missing in the  $2DL_1$  model. Indeed, in addition to the three previously discussed STM conditions, the low formation energy *FE* condition should also be fulfilled for a model to be a reasonable candidate to explain this reconstruction. As demonstrated by previously published models,<sup>3-7</sup> that also have failed to reproduce one or the other condition, meeting all the constraints in a model is a challenge.

To raise to this challenge, it is necessary to explore a wide range of possible configurations. Figure 2(c) depicts the grand potential energy for the more than 700 models considered in our study, demonstrating the potential richness of this surface. Colorized lines in Fig. 2(c) highlight the models with the lower formation energy in a given chemical potential window. These lower bound models fulfill by definition the *FE* condition. Indeed, the  $2DL_1$  model is the one with lower *FE* at  $\mu_C - E_C^{\text{bulk}} = 0$ , where it is also close in energy with the  $(2 \times 2)_C$  phase (model  $DA_1$  in the plot).<sup>16</sup> It has been observed<sup>17</sup> that the latter is in coexistence with the  $3 \times 3$  when they are formed in ultrahigh vacuum around 1075°C.

We also colorize the three significant models of literature that claim to reproduce the  $3 \times 3$  reconstruction but failed either for thermodynamics reasons<sup>3,7</sup> or STM incompatibility.<sup>6</sup> The model proposed by Nemeč *et al.*<sup>6</sup> ( $3DL_1$  in Fig. 2(c)) is interesting as it was the first to be a pure silicon structure that turns out to have a large stability range compatible with that of the bulk SiC. This team has pursued its search and independently proposed the same ad-layer  $2DL_1$  as a possible candidate for the  $3 \times 3$ .<sup>18</sup>

In order to understand why the  $2DL_1$  silicon over-layer does not reproduce the  $stm_g$  condition it is necessary to analyze the interaction of this layer with the last carbon layer. Among the nine dangling bonds in the  $3 \times 3$  cell, two are passivated by the silicon ad-atoms in top position (*A* and *B* sites), six are passivated by the three bridging Si connecting (*O* sites), the remaining dangling bond (*C* site) being not passivated. These atoms present a large peak in the DOS at the Fermi level (not shown) associated to their half-filled dangling-bond.

Pursuing with our analogy with the silica over-layer for which we recently got more insight,<sup>19</sup> we build a supercell of the  $2DL_1$  where some of the carbon atoms at the *C* site are substituted by silicon atoms. The calculations are done in a  $9 \times 6$  orthorhombic supercell containing 12 *C* sites that allow a substitution ranging from 25 to 66%. The formation energy for different ratios of silicon substitution is depicted in the inset of Fig. 2(c): from a thermodynamic point of view, these

substitutions at the  $C$  site are less stable than the parent  $2DL_1$  and can thus be viewed as defective.

In order to observe the effect of these substitutions on the STM images at energies close to zero bias, we make use of a smaller supercell, because we find that the contrast in the simulated  $stm_u$  image is quite sensitive to the thickness of the slab. Therefore, in a  $3 \times 3$  orthorhombic supercell with twice the thickness of our original  $4H$ -SiC slab, we recalculate a model with 50% of substitution. Thus, the model contains only two inequivalent  $C$  sites [Fig. 3(d)]. The corresponding STM simulations are depicted in Fig.3(a-c) together with the partial DOS for the surface atoms lying at the four characteristic sites  $A$ ,  $B$ ,  $C$  and  $O$  in panel (e).

In the partial DOS, we observe a change in the charge transfer on one hand between the carbon atom and the silicon atom at both  $C$  sites, and on the other hand between the both atoms at  $C$  sites and the silicon over-layer. Interestingly, a new state appears in the gap due to the silicon atom substituting one of the carbon atom at the  $C$  site. The energy range of this silicon state is broad and centered around  $-0.6\text{V}$ . More precisely, this  $-0.6\text{V}$  state corresponds to  $p_x$  and  $p_y$  orbitals hybridized with the three neighboring silicon atoms. The state at the Fermi level is of  $s$  and  $p_z$  character. The simulated STM image at  $-0.6\text{V}$  [Fig. 3(c)] clearly allows to assign this Si defect at  $C$  site as the  $C^+$  defect observed by Hiebel *et al.*<sup>5,9</sup> Subsequently, the  $C^-$  sites are ascribed to the last carbon atom presenting a dangling bond in the parent  $2DL_1$  model. Interestingly, the carbon atoms at the  $C^-$  sites are drawn towards the surface whereas silicon atoms at the  $C^+$  sites relax outward it [Fig. 3d] with a height difference of  $0.5\text{\AA}$  between both sites. This height difference is consistent with differences observed in the profile lines from STM images ( $\approx 0.4$  and  $0.5\text{\AA}$  in the Fig. 1(c) in Ref. 5) further confirming the present assignment of  $C^+$  and  $C^-$  sites. This small difference, moreover, has an impact in the low intensity values of the these sites in the simulated STM image at  $-2.5\text{V}$  [Fig. 3(a)]. This is also confirmed by the experimental topographies (Fig. 1(b) of Ref. 5).

Finally, the disorder seems to derive from the complex charge transfer between  $C^+$  and  $C^-$  sites and the over-layer. In order to introduce the idea of disorder, we have to acknowledge that the charge transfer is incomplete as some electrons stay on  $C^-$  sites, leading to a peak at the Fermi level. We infer that this comes from a complex balance of the electron in the over-layer on one hand and in the substitutional silicon at  $C^+$  site on the other hand. This is an important point for graphene growth as this over-layer is interfaced with graphene. The occurrence of such a disorder at  $C$  sites in the experimental STM [Fig. 1(c)] is an additional proof that a perfect passivation coming from complete charge transfer can not be found in a finite size super-cell.

To get more insight on the physics of the charge transfer between  $C$  sites, we substitute in the  $3\times 3$  super-cell one of the two carbon atoms at  $C$  sites by a Ga atom and the second one by an As atom. This choice being driven by the reminiscence of the topology of the  $C^+$  and  $C^-$  sites with these of a  $\langle 110 \rangle$  GaAs surface<sup>20</sup>. In this well documented surface reconstruction case, the difference of electronegativity between Ga and As atoms drives a charge transfer from Ga to As sites leading to a Ga atom with a quasi  $sp^2$  configuration (with a empty  $p_z$  orbital) and an As atom with a quasi  $sp^3$  configuration that displays a lone pair. Such a charge transfer leading to a self-reconstruction of all the dangling bonds. As a matter of fact, we found that such a complete charge transfer also occurs between the Ga-substituted  $C$  site and the As-substituted one (as calculated by a Bader analysis<sup>21</sup>). The corresponding topologies match those of  $C^+$  and  $C^-$  for As and Ga atoms respectively. In the case of silicon substituted  $C$  sites, the charge transfer occurs but only partially as already discussed. We suspect that this partial charge transfer comes from a competition between the two following properties: a larger bond length for Si-Si with respect to C-Si and a lower electronegativity for silicon with respect to C. Indeed, the first property drive Si-substituted  $C$  site to a  $C^+$  topology while the second property drive them to the  $C^-$  one thus leading the whole system to an incommensurate charge transfer in our two  $C$  sites supercell. This analysis is consistent with the experimental ratio of  $C^+$  sites being  $\approx 65\%$ , as indeed a 50% ratio would correspond to a full and commensurate charge transfer as in the case of Ga and As substitution.

In summary, based on a extensive exploration of the surface PES, we propose an energetically-favorable atomic model that reproduces for the first time the three main STM *conditions* reported for the  $3\times 3$  reconstruction of the C-face of SiC.<sup>5</sup> This model is close to that of the silica overlayer grown on Ru oxide.<sup>15</sup> It forms an all-silicon honeycomb-kagome network at the surface of a  $3\times 3$  supercell that passivate 8 over the 9 carbon dangling bonds in the supercell. The last carbon dangling bond is passivated through a charge transfer between Si-substituted sites and un-substituted one. This charge transfer is, however, not commensurate with the lattice due to a competition between the bond length and the electronegativity of silicon with respect to C. This competition explains the disordered character in the two different types of  $C$  sites, thus leading to a strong disorder below the highly ordered  $3\times 3$  overlayer.

## ACKNOWLEDGMENTS

E.MC, LM, NM and PP acknowledge financial support from the NanoScience Foundation. NM also acknowledge financial support from the Natural Sciences and Engineering Research Council of Canada. CG acknowledges financial support by Spanish government through project MAT2017-88258-R and the “María de Maeztu” Program for Units of Excellence in R&D (MDM-2014-0377). The BigDFT calculations were done using French supercomputers (GENCI) through Project 6194 and the supercomputers of Calcul Québec/Compute Canada. E.MC and PP acknowledge stimulating discussions with Dr. Fanny Hiebel, Dr. Jean-Yves Veuillen and Dr. Pierre Mallet and their valuable collaboration.

## REFERENCES

- <sup>1</sup>G. P. Srivastava, Reports on Progress in Physics **60**, 561 (1997).
- <sup>2</sup>C. Brun, T. Cren, and D. Roditchev, Superconductor Science and Technology **30**, 013003 (2016).
- <sup>3</sup>H. E. Hoster, M. A. Kulakov, and B. Bullemer, Surface Science **382**, L658 (1997).
- <sup>4</sup>L. Li and I. S. T. Tsong, Surface Science **351**, 141 (1996).
- <sup>5</sup>F. Hiebel, L. Magaud, P. Mallet, and J. -Y. Veuillen, Journal of Physics D: Applied Physics **45**, 154003 (2012).
- <sup>6</sup>L. Nemeč, F. Lazarevic, P. Rinke, M. Scheffler, and V. Blum, Physical Review B **91**, 161408(R) (2015).
- <sup>7</sup>I. Deretzis and A. La Magna, Applied Physics Letters **102**, 093101 (2013).
- <sup>8</sup>F. Hiebel, P. Mallet, F. Varchon, L. Magaud, and J. -Y. Veuillen, Solid State Communications **149**, 1157 (2009).
- <sup>9</sup>F. Hiebel, *Investigation of the graphene - SiC(000-1) (carbon face) interface using scanning tunneling microscopy and ab initio numerical simulations*, Ph.D. thesis, Univ. Grenoble Alpes (2011).
- <sup>10</sup>E. Machado-Charry, L. K. Béland, D. Caliste, L. Genovese, T. Deutsch, N. Mousseau, and P. Pochet, The Journal of Chemical Physics **135**, 034102 (2011), <https://doi.org/10.1063/1.3609924>.
- <sup>11</sup>S. De, A. Willand, M. Amsler, P. Pochet, L. Genovese, and S. Goedecker, Phys. Rev. Lett. **106**,



- 225502 (2011).
- <sup>12</sup>L. Genovese, A. Neelov, S. Goedecker, T. Deutsch, S. A. Ghasemi, A. Willand, D. Caliste, O. Zilberberg, M. Rayson, A. Bergman, and R. Schneider, *The Journal of Chemical Physics* **129**, 014109 (2008).
- <sup>13</sup>J. P. Lewis, P. Jelínek, J. Ortega, A. d. A. Demkov, D. G. Trabada, B. Haycock, H. Wang, G. Adams, J. K. Tomfohr, E. Abad, H. Wang, and D. A. Drabold, *physica status solidi (b)* **248**, 1989 (2011).
- <sup>14</sup>J. M. Blanco, C. González, P. Jelínek, J. Ortega, F. Flores, and R. Pérez, *Phys. Rev. B* **70**, 085405 (2004).
- <sup>15</sup>S. Mathur, S. Vlaic, E. Machado-Charry, A.-D. Vu, V. Guisset, P. David, E. Hadji, P. Pochet, and J. Coraux, *Physical Review B* **92**, 161410(R) (2015).
- <sup>16</sup>L. Magaud, F. Hiebel, F. Varchon, P. Mallet, and J. -Y. Veuillen, *Physical Review B* **79**, 161405(R) (2009).
- <sup>17</sup>J. Hass, W. A. de Heer, and E. H. Conrad, *Journal of Physics: Condensed Matter* **20**, 323202 (2008).
- <sup>18</sup>J. Li, Q. Wang, G. He, M. Widom, L. Nemeč, V. Blum, M. Kim, P. Rinke, and R. M. Feenstra, *Phys. Rev. Materials* **3**, 084006 (2019).
- <sup>19</sup>G. Kremer, J. C. Alvarez Quiceno, S. Lisi, T. Pierron, C. González, M. Sicot, B. Kierren, D. Malterre, J. E. Rault, P. Le Fèvre, F. i. Bertran, Y. J. Dappe, J. Coraux, P. Pochet, and Y. Fagot-Revurat, *ACS Nano* **13**, 4720 (2019), pMID: 30916924.
- <sup>20</sup>G.-X. Qian, R. M. Martin, and D. J. Chadi, *Phys. Rev. B* **37**, 1303 (1988).
- <sup>21</sup>W. Tang, E. Sanville, and G. Henkelman, *Journal of Physics: Condensed Matter* **21**, 084204 (2009).
- <sup>22</sup>S. Mathur, *Growth and atomic structure of a novel crystalline two-dimensional material based on silicon and oxygen*, Ph.D. thesis, Univ. Grenoble Alpes (2016).

## FIGURE CAPTIONS

FIG. 1. The SiC  $3 \times 3$  (cyan rhombus) reconstruction. STM at different voltages; (a)  $stm_o$  at  $-2.5V$ , (b)  $stm_u$  at  $2.5V$  and (c)  $stm_g$  at  $-0.65V$ .<sup>9</sup> (d) STM of ultra-thin silica on  $2 \times 2$  (green rhombus) Ru oxide measured at  $0.9V$ .<sup>22</sup> (e-f) This film is composed of two Si ad-atoms respectively on a top and an hollow Ru positions<sup>15</sup> and 3 bridging O atoms (defining  $O$  sites). Si, O and Ru atoms are blue, red and purple respectively. The  $2DL_1$  model (g-h) contains 2 top Si ad-atoms on  $A$  and  $B$  sites and 3 bridging Si on  $O$  sites. These five ad-atoms forming an over-layer are shown in blue and their connections with the carbon dangling bonds are represented by red bonds, whereas bulk Si and C atoms are green and black. STM simulations of  $2DL_1$  at  $-2.5V$  (i) and  $+2.5V$  (j) to be compared to (a) and (b) respectively.

FIG. 2. The intensive PES exploration of the  $3 \times 3$  SiC surface. (a) Scatter plot of evaluated models as a function of the surplus at the surface of C and Si atoms with respect to the raw bulk-terminated surface  $3 \times 3$ . Negative values means removal of atoms from the sub-surface layer. The radius of each circle is proportional to the number of considered models at a given surface chemistry. The dotted lines correspond to a full addition/removal of atoms of the same type in the last SiC bilayer. Closed contours correspond to sectors of a given topology class for the lowest  $FE$  model at each concentration point. Color is scaled on formation energy at  $\Delta\mu_C = 0$  in reference to the lowest energy model, i.e. the  $2DL_1$  one at  $(0,5)$ . (b) A schematic view of examples for the five class of topologies: pure ad-atoms, 2D and 3D Cluster of ad-atoms, 2D and 3D ad-Layers covering the whole surface. Si and C atoms are in red and gray respectively. (c) surface formation energy ( $FE$ ) as a function of the carbon chemical potential.  $FE$  was calculated relative to the raw bulk-terminated SiC surface ( $1 \times 1$ ). The SiC bulk is stable in the range  $-0.628 \leq \mu_C - E_C^{\text{bulk}} \leq 0$  eV. Some previous models are:  $3DL_1$  (blue),<sup>6</sup>  $3DC_2$  (lime green)<sup>7</sup> and  $3DC_1$  (dark red).<sup>3</sup>

FIG. 3. STM images of a  $2DL_1$  supercell with 50% silicon substituted C sites at different voltages: (a)  $-2.5V$ , (b)  $2.5V$  and (c)  $-0.6V$ . The five different site types are marked by colored circles:  $A$  (orange),  $B$  (green),  $C^+$  (light blue),  $C^-$  (dark blue) and  $O$  sites (red). The surface cell of the  $3 \times 3$  is represented by a cyan rhombus. (d) 3D view of the surface with the color marks used in a-c

panels. (e) The partial DOS for the five type of atoms highlighted in (d). Color lines follow the same color code as in (d).

FIG. 4.

## FIGURES

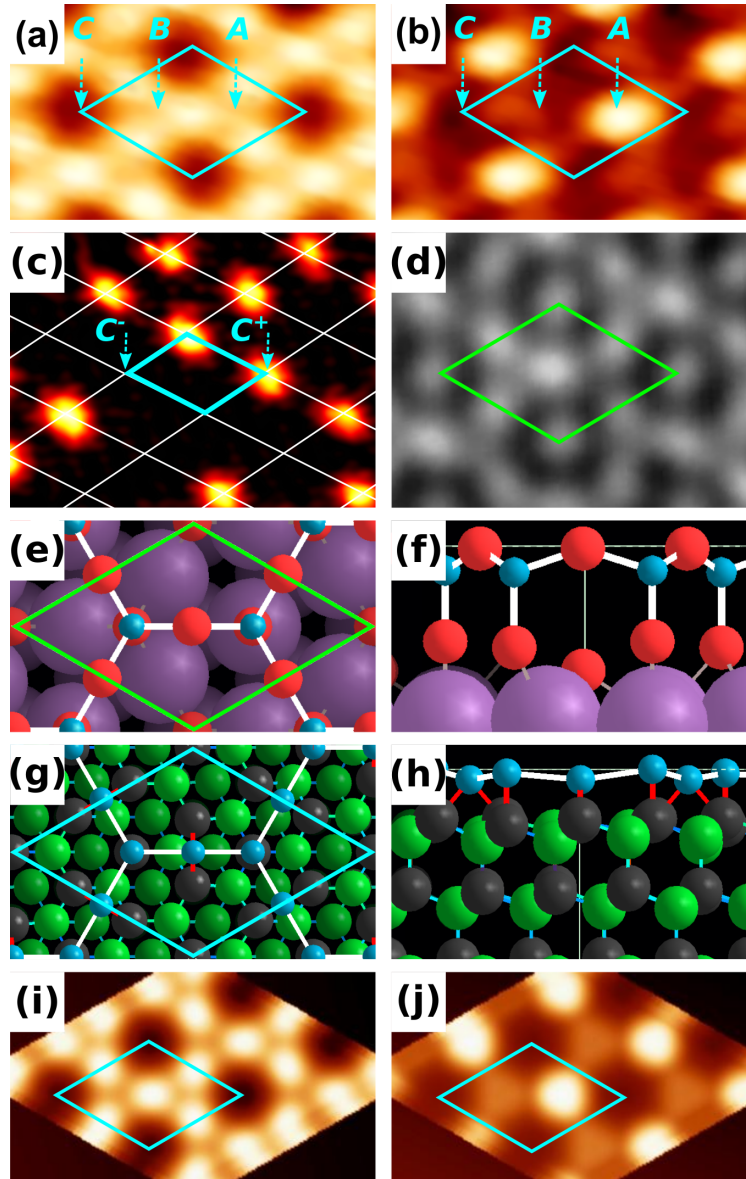


FIG. 1. The SiC  $3 \times 3$  (cyan rhombus) reconstruction. STM at different voltages; (a)  $stm_o$  at  $-2.5V$ , (b)  $stm_u$  at  $2.5V$  and (c)  $stm_g$  at  $-0.65V$ .<sup>9</sup> (d) STM of ultra-thin silica on  $2 \times 2$  (green rhombus) Ru oxide measured at  $0.9V$ .<sup>22</sup> (e-f) This film is composed of two Si ad-atoms respectively on a top and an hollow Ru positions<sup>15</sup> and 3 bridging O atoms (defining O sites). Si, O and Ru atoms are blue, red and purple respectively. The  $2DL_1$  model (g-h) contains 2 top Si ad-atoms on A and B sites and 3 bridging Si on O sites. These five ad-atoms forming an over-layer are shown in blue and their connections with the carbon dangling bonds are represented by red bonds, whereas bulk Si and C atoms are green and black. STM simulations of  $2DL_1$  at  $-2.5V$  (i) and  $+2.5V$  (j) to be compared to (a) and (b) respectively.

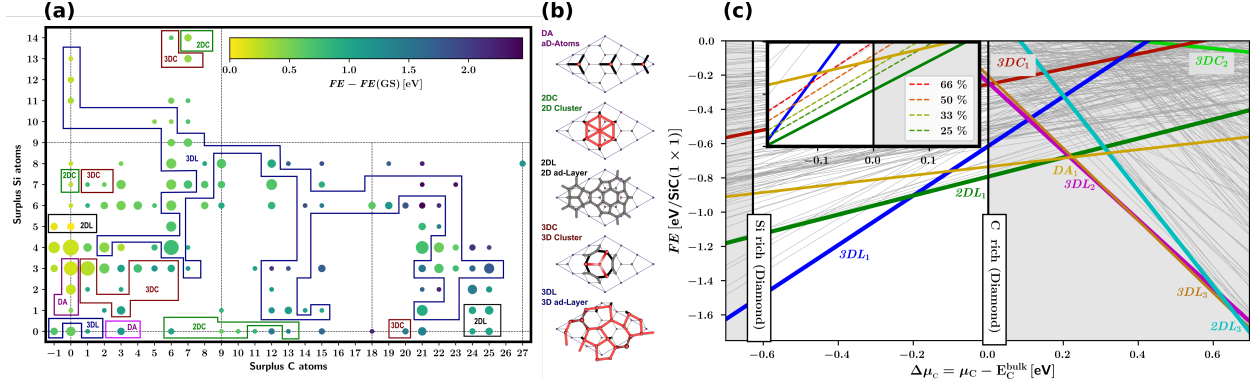


FIG. 2. The intensive PES exploration of the  $3 \times 3$  SiC surface. (a) Scatter plot of evaluated models as a function of the surplus at the surface of C and Si atoms with respect to the raw bulk-terminated surface  $3 \times 3$ . Negative values means removal of atoms from the sub-surface layer. The radius of each circle is proportional to the number of considered models at a given surface chemistry. The dotted lines correspond to a full addition/removal of atoms of the same type in the last SiC bilayer. Closed contours correspond to sectors of a given topology class for the lowest  $FE$  model at each concentration point. Color is scaled on formation energy at  $\Delta\mu_C = 0$  in reference to the lowest energy model, i.e. the  $2DL_1$  one at (0,5). (b) A schematic view of examples for the five class of topologies: pure ad-atoms, 2D and 3D Cluster of ad-atoms, 2D and 3D ad-Layers covering the whole surface. Si and C atoms are in red and gray respectively. (c) surface formation energy ( $FE$ ) as a function of the carbon chemical potential.  $FE$  was calculated relative to the raw bulk-terminated SiC surface ( $1 \times 1$ ). The SiC bulk is stable in the range  $-0.628 \leq \mu_C - E_C^{\text{bulk}} \leq 0$  eV. Some previous models are:  $3DL_1$  (blue),<sup>6</sup>  $3DC_2$  (lime green)<sup>7</sup> and  $3DC_1$  (dark red).<sup>3</sup>

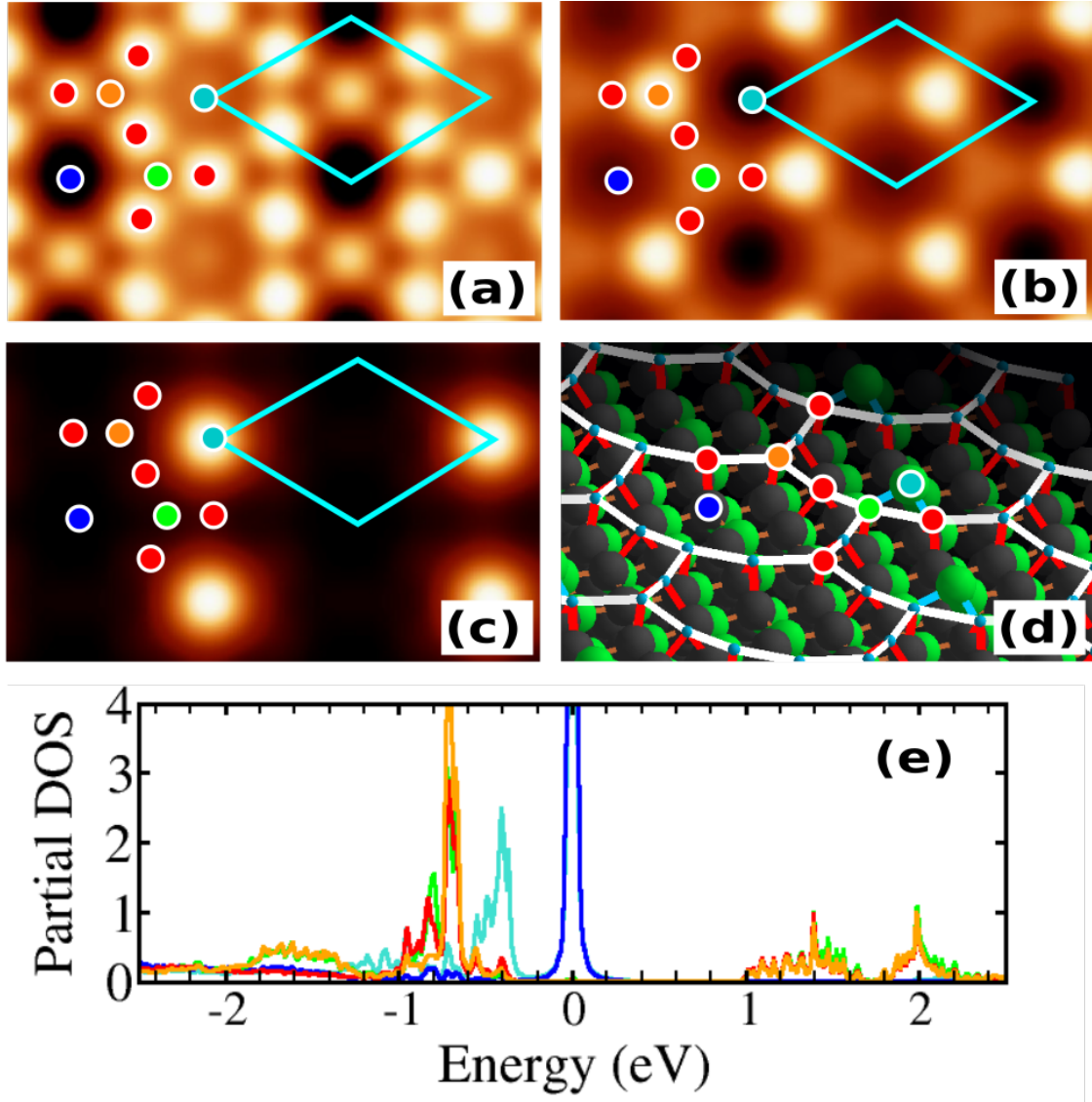


FIG. 3. STM images of a  $2DL_1$  supercell with 50% silicon substituted  $C$  sites at different voltages: (a) -2.5V, (b) 2.5V and (c) -0.6V. The five different site types are marked by colored circles:  $A$  (orange),  $B$  (green),  $C^+$  (light blue),  $C^-$  (dark blue) and  $O$  sites (red). The surface cell of the  $3 \times 3$  is represented by a cyan rhombus. (d) 3D view of the surface with the color marks used in a-c panels. (e) The partial DOS for the five type of atoms highlighted in (d). Color lines follow the same color code as in (d).

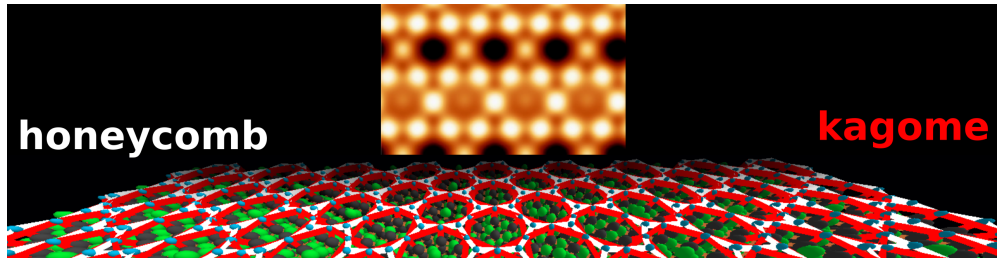


FIG. 4.

Graphical TOC Graphical TOC